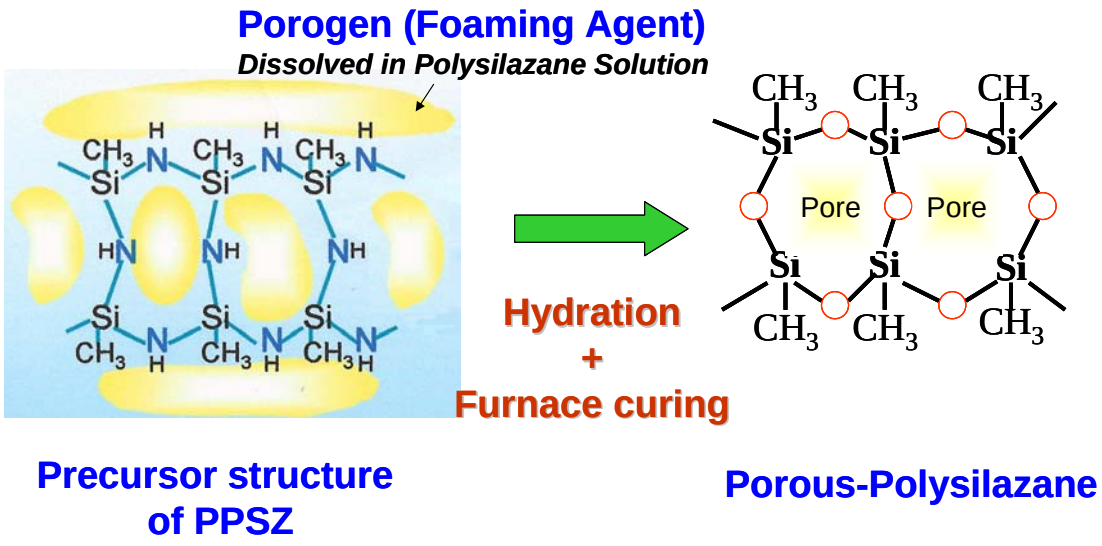

Figure 3-1 Method of precursor structure transfer to final porous-polysilazane (PPSZ) structure.

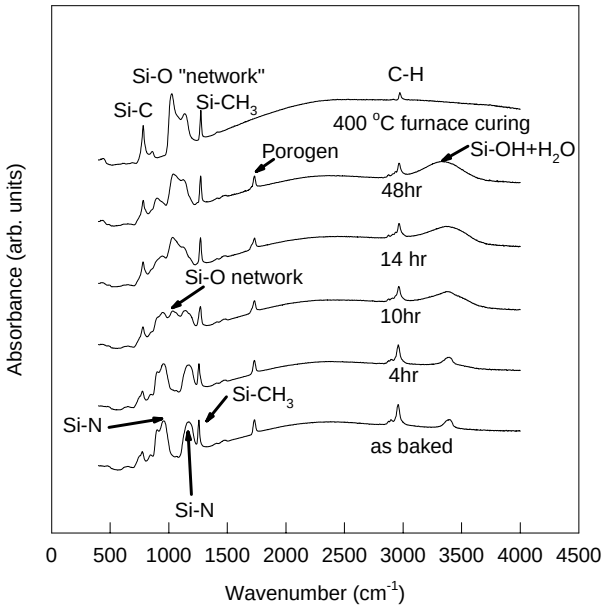

Figure 3-2 FTIR spectra of PPSZ film during formation.

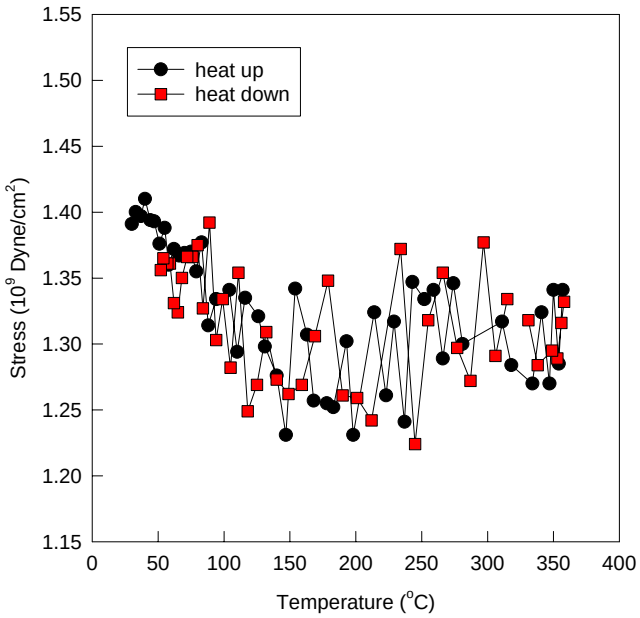

Figure 3-3 The internal stress variation of PPSZ during thermal cycle.

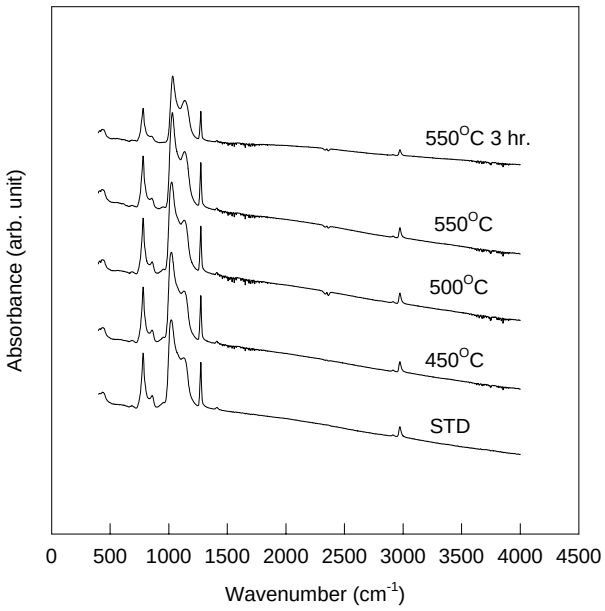

Figure 3-4 FTIR spectra of PPSZ films after various thermal annealing temperature.

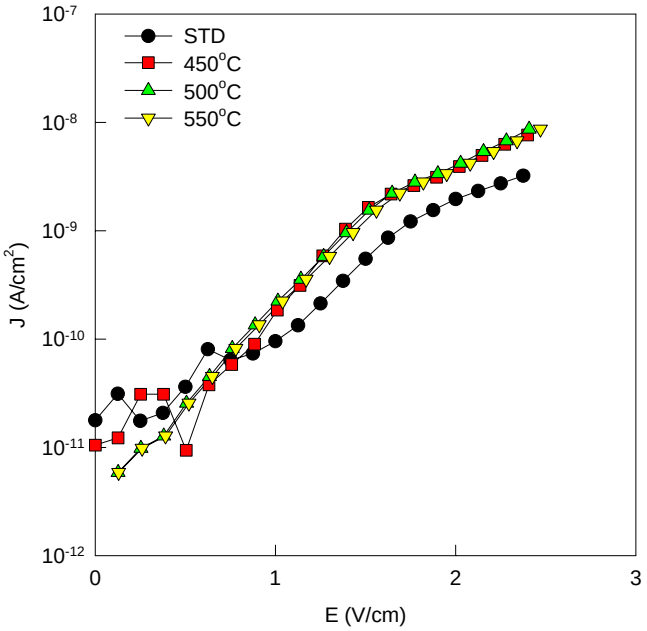

(a)

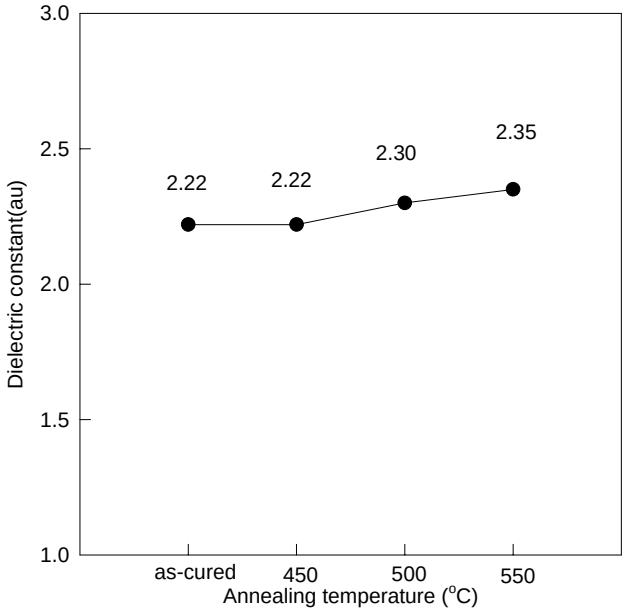

(b)

Figure 3-5 Dielectric properties of the PPSZ film after thermal annealed at various temperature (a) leakage current density of the PPSZ versus electric field (b) dielectric constant of the PPSZ films versus annealing temperature.

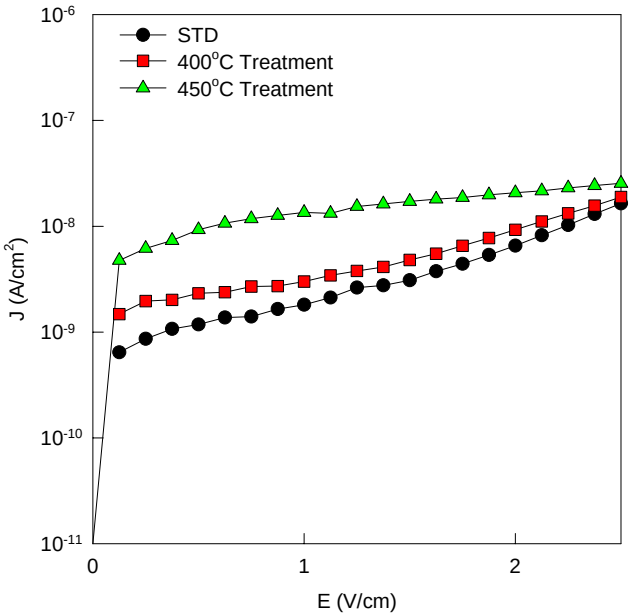

Figure 3-6 The leakage current density of temperature dependence of thermal stress for Cu electrode MIS structure.

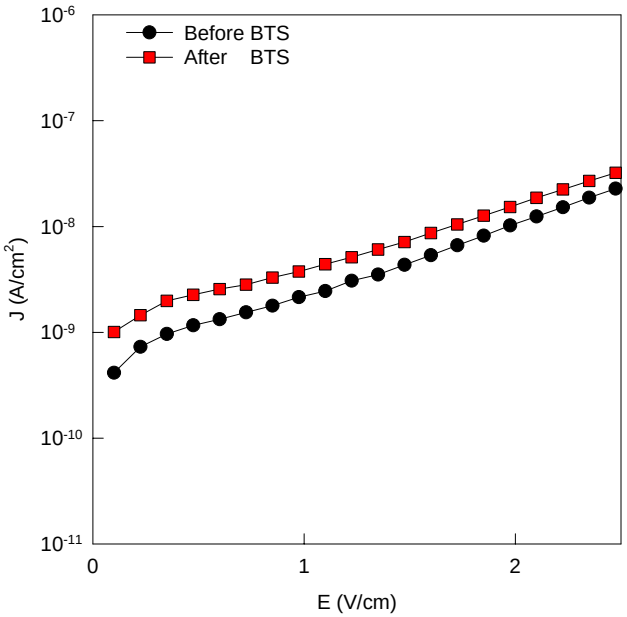

Figure 3-7 Comparison of leakage current density of PPSZ before and after BTS stress at 190 °C and 2 MV/cm for 1000 sec.

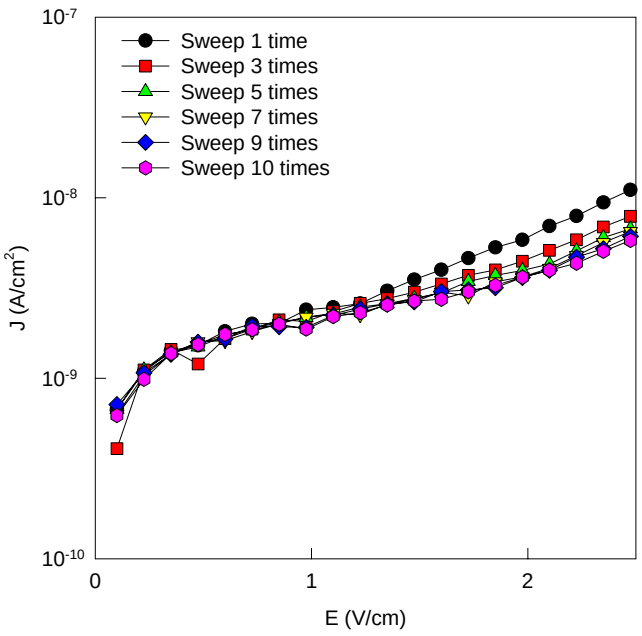

Figure 3-8 J-E curves performed with different sweeping times. It is found that the leakage current is decreased with increasing sweeping times.

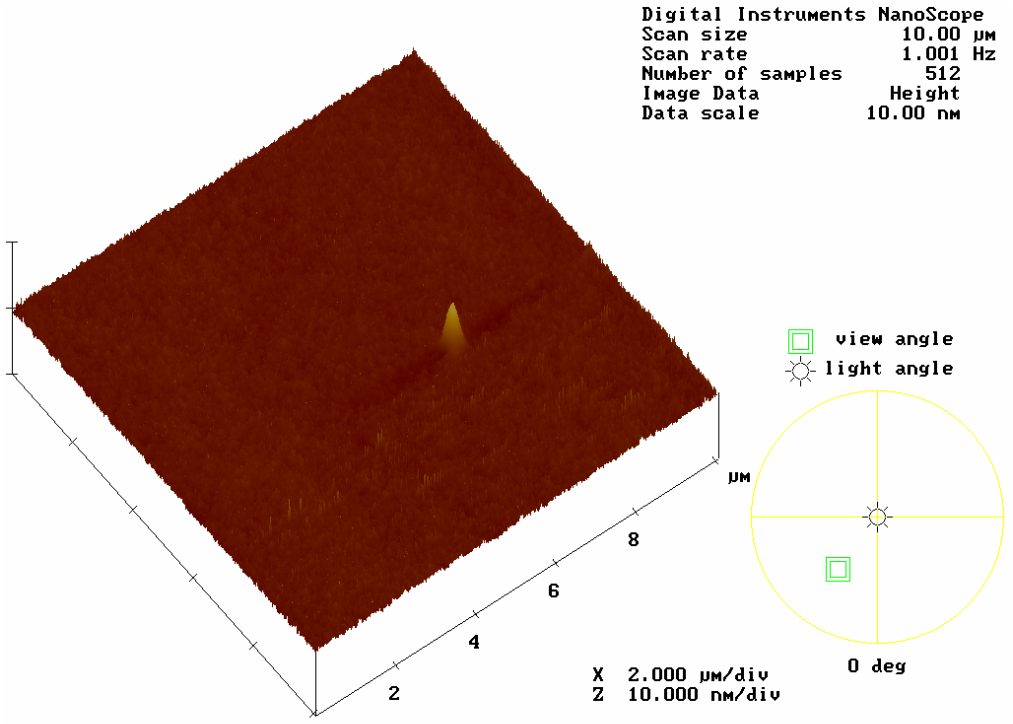

(a)

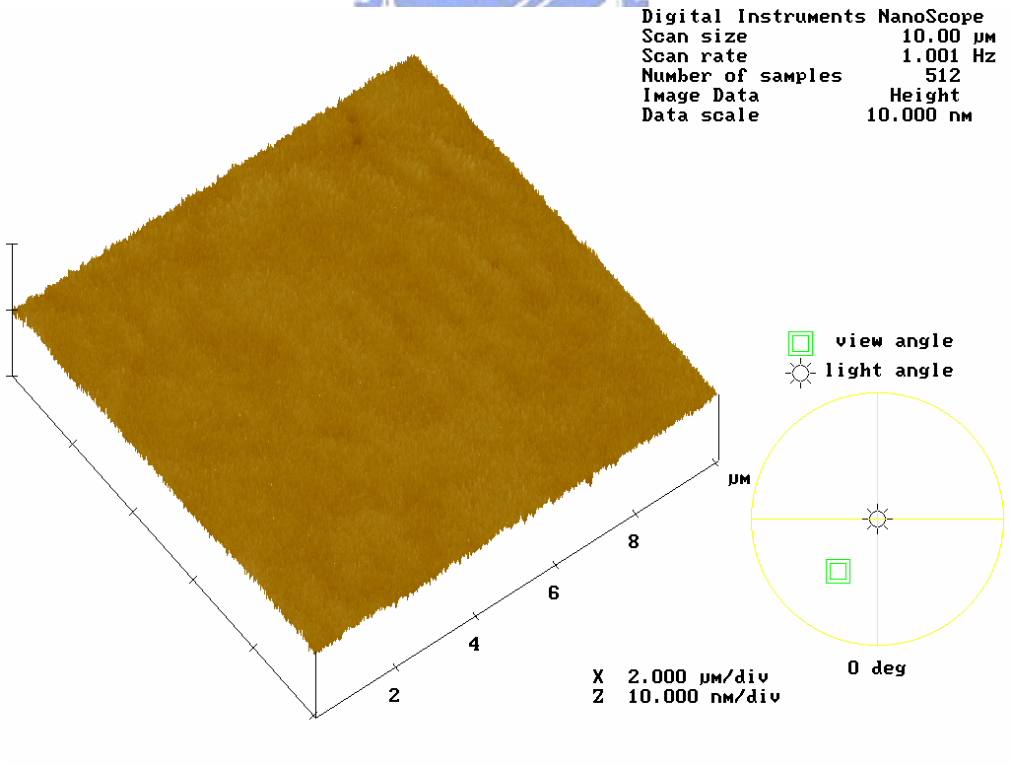

(b)

Figure 3-9 AFM image surface of polished PPSZ (a) with TaN slurry (b) with Cu slurry.

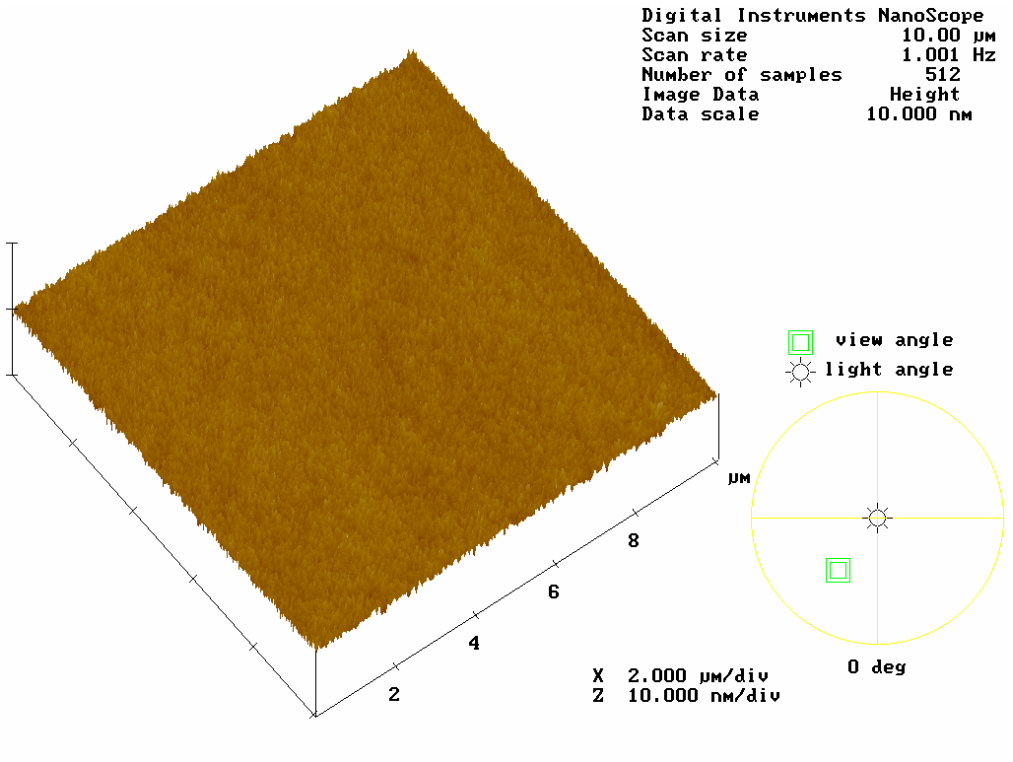

Figure 3-10 AFM micrograph surface of polished PPSZ with commercial SS-25 slurry.

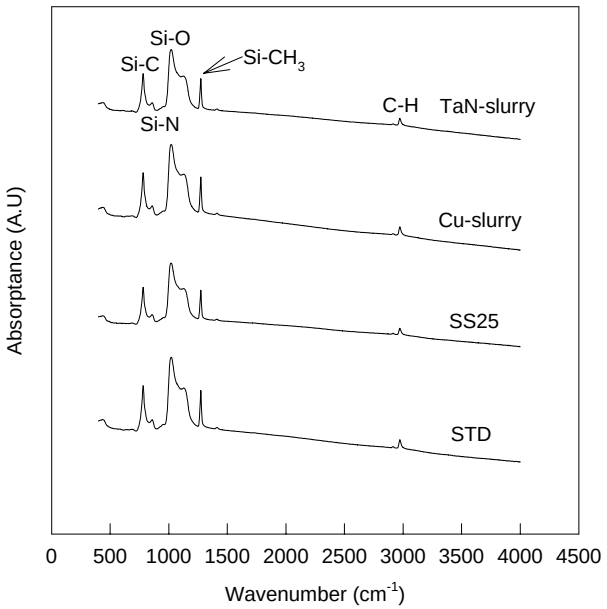

Figure 3-11 FTIR Spectra of post-CMP PPSZ with various slurries.

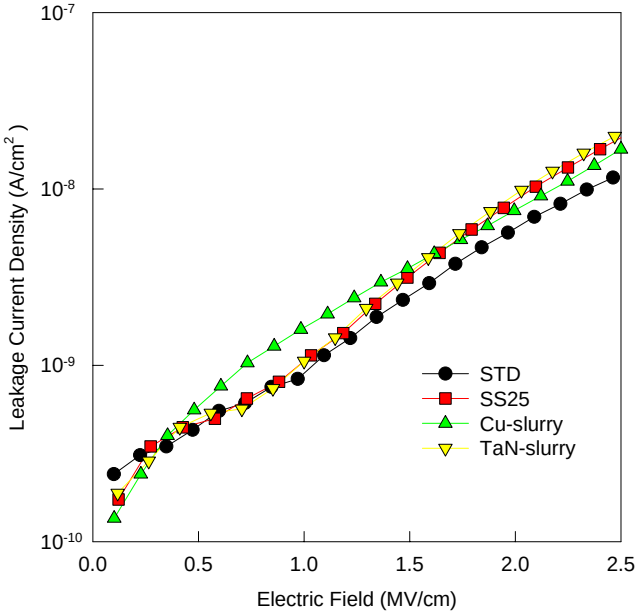

(a)

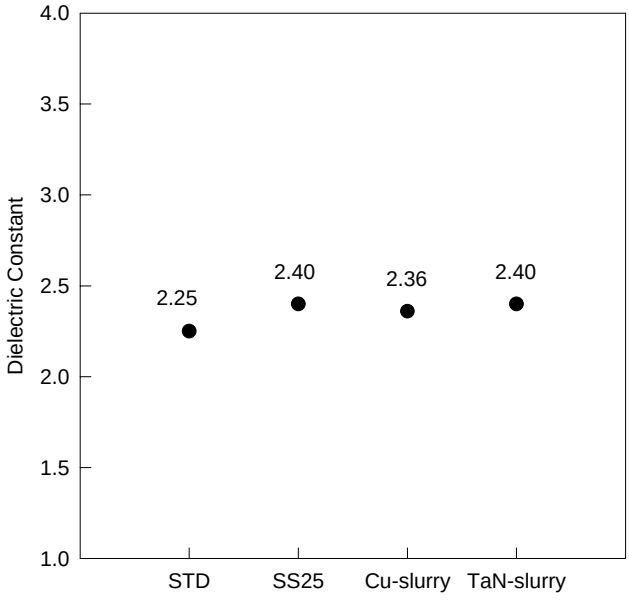

(b)

Figure 3-12 Dielectric properties of PPSZ films polished with various slurries: (a) leakage current density of post-CMP PPSZ films versus electric field (b) dielectric constants of post-CMP PPSZ films.

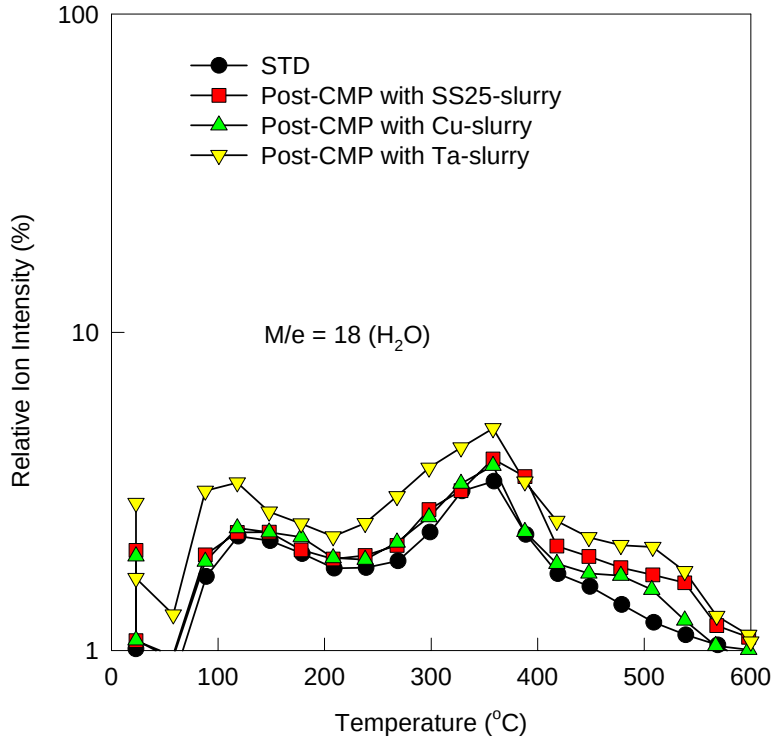

Figure 3-13 The TDS moisture desorption spectra of PPSZ polished with various Slurries

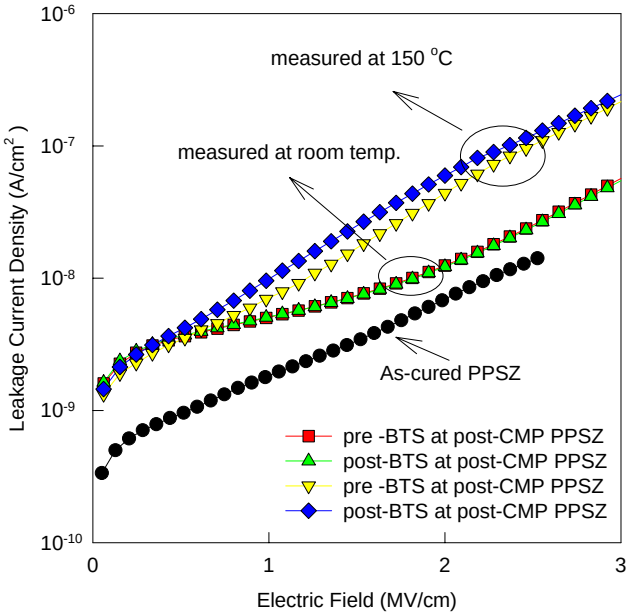
measured at 150 °C
measured at room temp.
As-cured PPSZ
pre -BTS at post-CMP PPSZ
post-BTS at post-CMP PPSZ
pre -BTS at post-CMP PPSZ
post-BTS at post-CMP PPSZ
Leakage Current Density (A/cm2)
Electric Field (MV/cm)
10-6
10-7
10-8
10-9
10-10
0
1
2
3

(a)

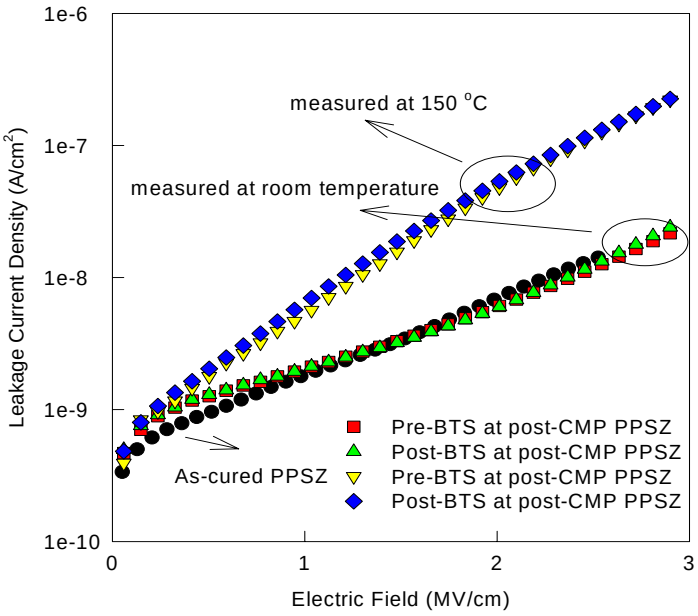
measured at 150 °C
measured at room temperature
As-cured PPSZ
Pre-BTS at post-CMP PPSZ
Post-BTS at post-CMP PPSZ
Pre-BTS at post-CMP PPSZ
Post-BTS at post-CMP PPSZ
Leakage Current Density (A/cm2)
Electric Field (MV/cm)
1e-6
1e-7
1e-8
1e-9
1e-10
0
1
2
3

(b)

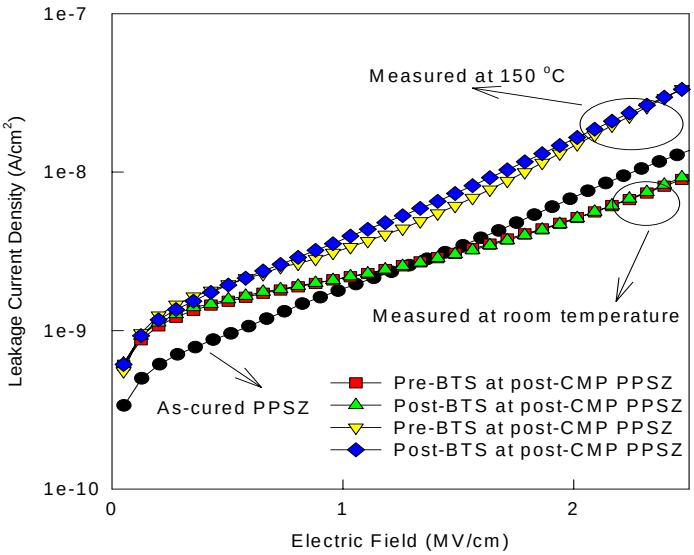

(c)

Figure 3-14 Leakage current density of Cu-electrode polished PPSZ film after 2 MV/cm at 150 °C for 1000 sec BTS stress measured at room temperature and 150 °C (a) with SS-25 Slurry (b) with TaN Slurry (c) with Cu slurry.

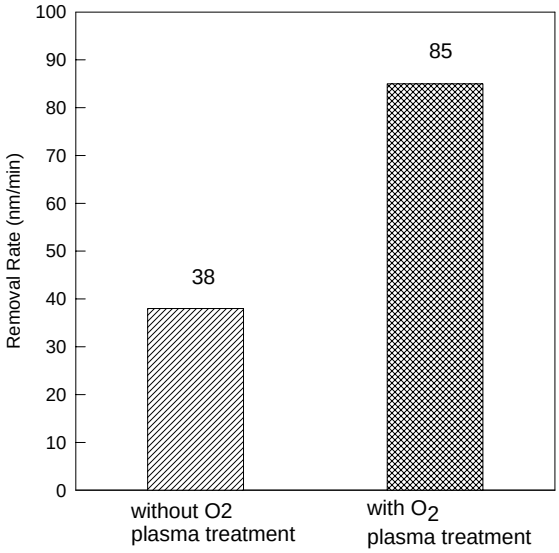

Figure 3-15 Removal rate of CMP with and without O_2 plasma pre-treatment.

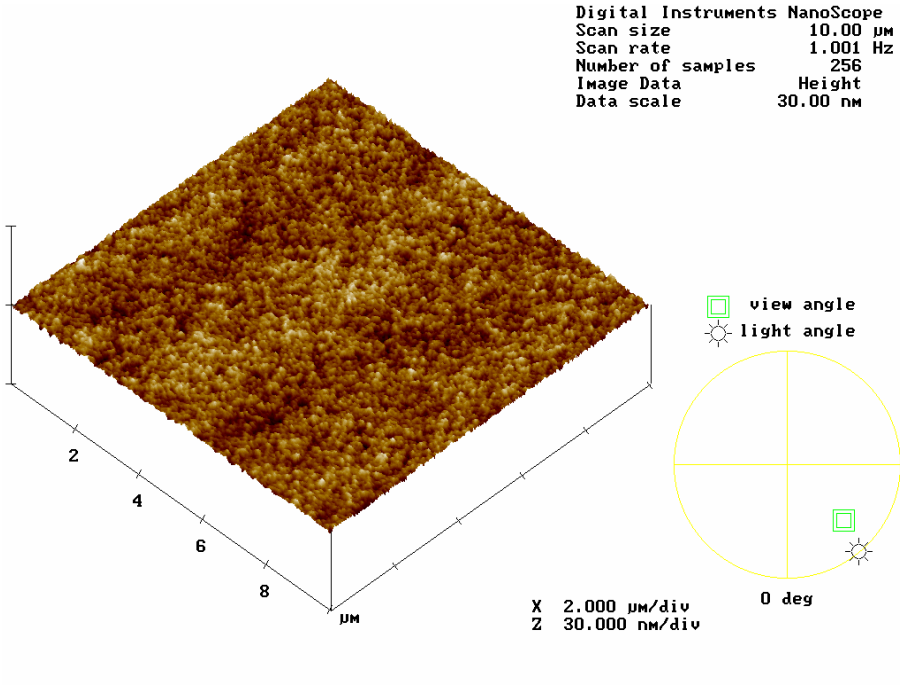

(a)

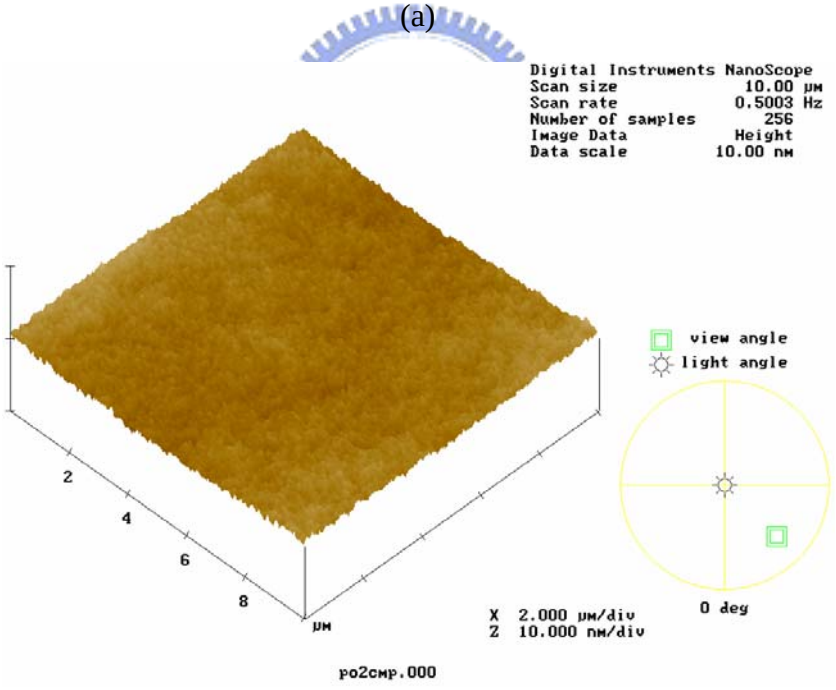

(b)

Figure 3-16 AFM micrographs of 30 sec O_2 plasma-treated PPSZ films (a) without CMP process (b) with CMP process.

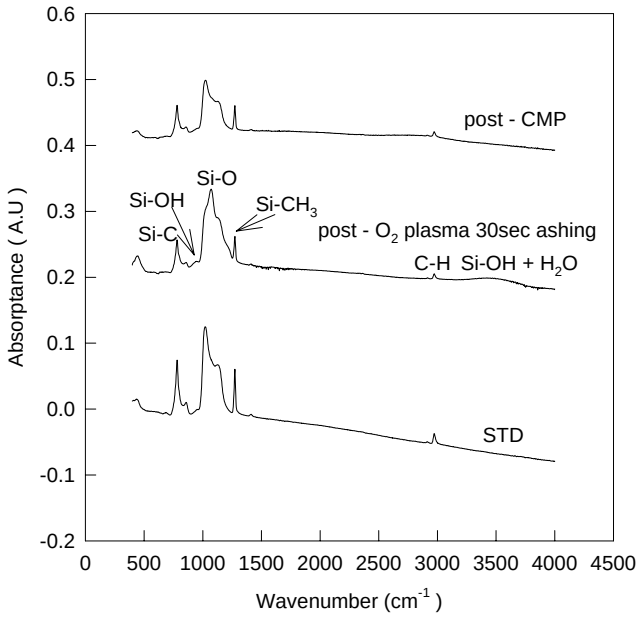

Figure 3-17 FTIR spectra of O_2 plasma-treated PPSZ films before and after CMP process.

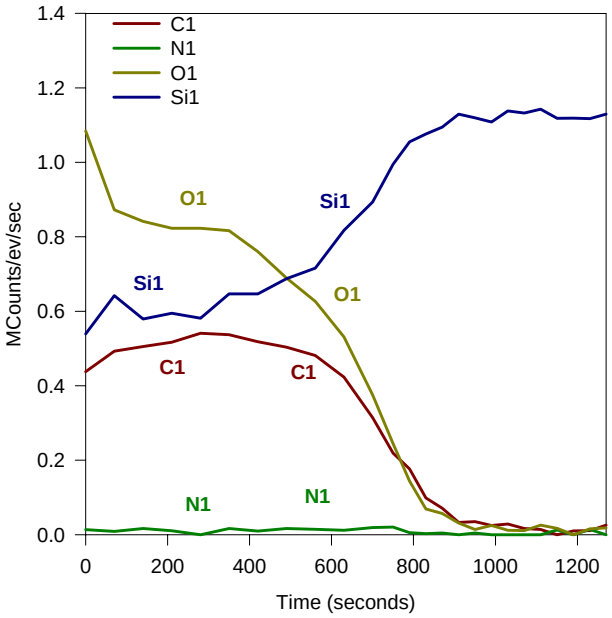

(a)

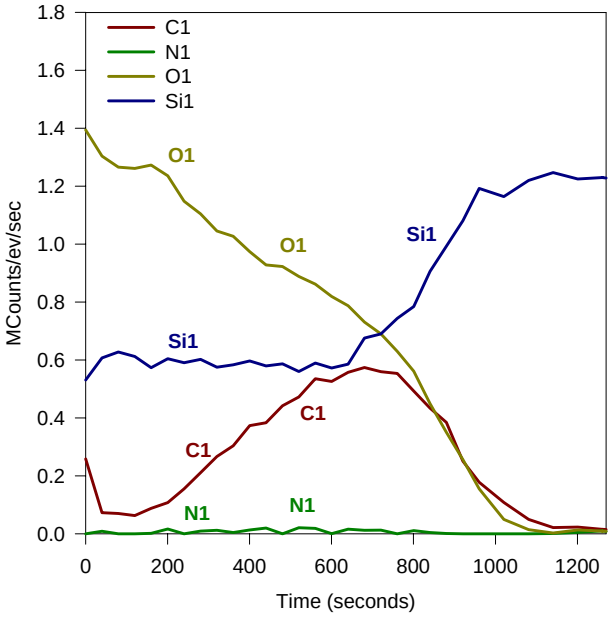

(b)

Figure 3-18 The auger depth profile of (a) as-cured PPSZ film (b) 45 sec O_2 plasma treated PPSZ film.

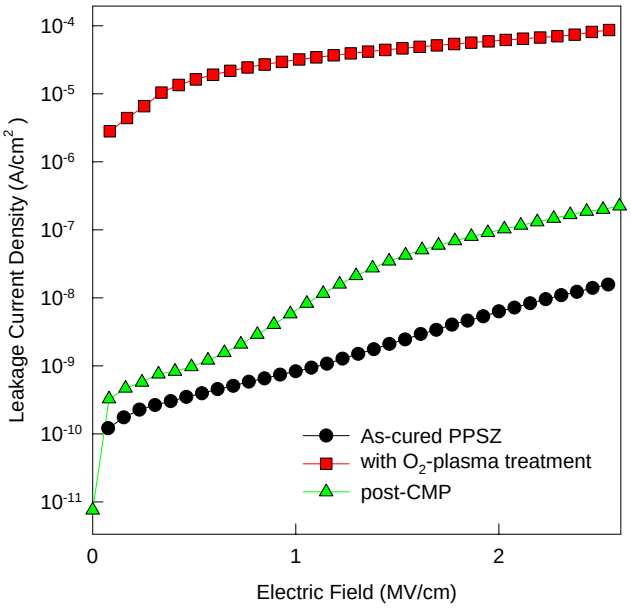

(a)

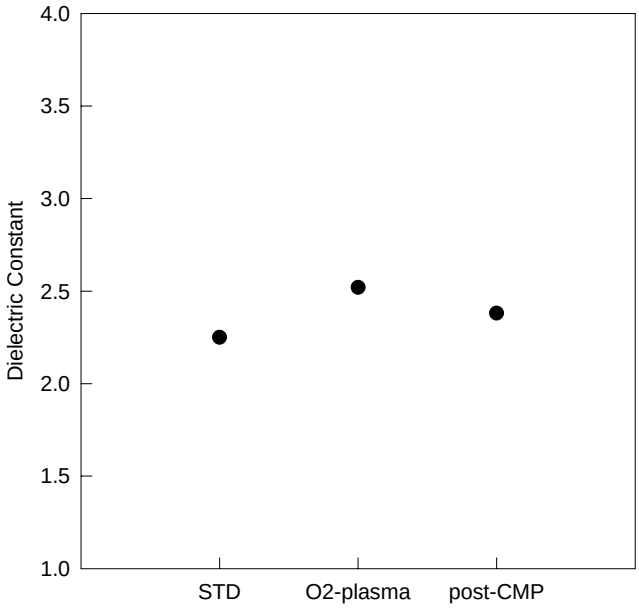

(b)

Figure 3-19 Dielectric properties of O_2 plasma-treated PPSZ before and after CMP process (a) leakage current density of PPSZ films versus electric field (b) variation in dielectric constant of PPSZ films.

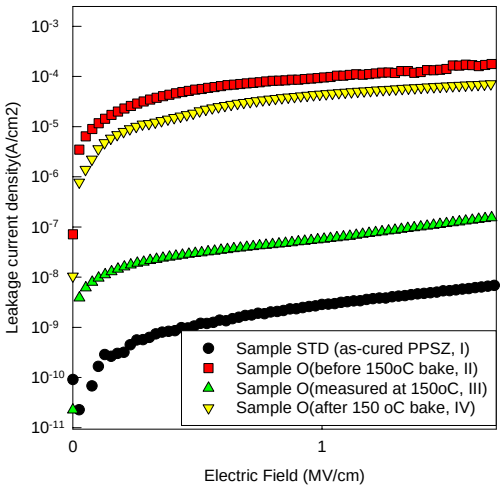

Figure 3-20 Leakage-current density of sample O before and after the 150 ^{o}C bake [curve I, sample STD measured at 25 ^{o}C; curve II, sample O measured at 25 ^{o}C (before 150 ^{o}C bake); curve III, sample O measured at 150 ^{o}C; curve IV, sample O measured at 25 ^{o}C (after 150 ^{o}C bake)].

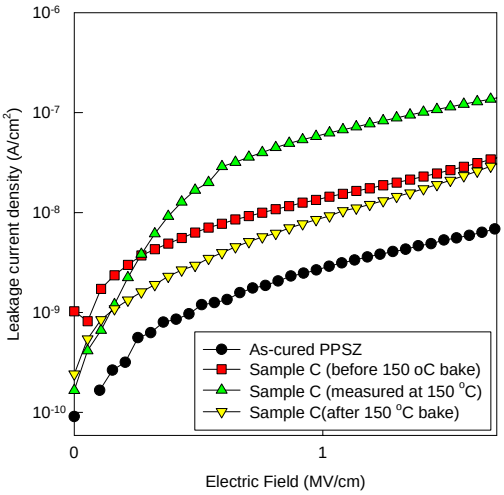

Figure 3-21 Leakage-current density of sample C before and after 150 ^{o}C bake [curve I, sample STD measured at 25 ^{o}C; curve II, sample C measured at 25 ^{o}C (before 150 ^{o}C bake); curve III, sample C measure at 150 ^{o}C; curve IV, sample C measured at 25 ^{o}C (after 150 ^{o}C bake)].